Role of Ca 2+ activation and bilobal structure of calmodulin in nuclear and nucleolar localization

Richard Thorogate, Katalin Török

Biochemical Journal Immediate Publication. Published on 16 Oct 2006 as manuscript BJ20061111

Role of Ca^{2+} activation and bilobal structure of calmodulin in nuclear and nucleolar localization

Richard Thorogate and Katalin Török*

Division of Basic Medical Sciences, St George's University of London, London, SW17 0RE

Corresponding author: Dr. K. Török
Division of Basic Medical Sciences, St George's University of London, Cranmer Terrace, London, SW17 0RE
Phone: +44 208 725 5832
Fax: +44 208 725 3581
e-mail: k.torok@sgul.ac.uk

Key words: CaM, nucleus, nucleolus, chromatin, calcium

Running title: CaM in the nucleus

Biochemical Journal Immediate Publication. Published on 16 Oct 2006 as manuscript BJ20061111

Ca^{2+} signaling to the nucleus is thought to occur by calmodulin entry into the nucleus where calmodulin has many functions. We investigated the role of Ca^{2+} and the N- and C-terminal lobes of calmodulin in its subnuclear targeting by using fluorescently labeled calmodulin and its mutants and confocal microscopy. Our data show, firstly, that Ca^{2+} stimulation induces a reorganization of subnuclear structures to which apo-calmodulin can bind. Secondly, Ca^{2+}-independent association of the C-terminal lobe is seen with subnuclear structures such as chromatin, the nuclear envelope and the nucleoli. Thirdly, Ca^{2+}-dependent accumulation of both calmodulin and the C-terminal calmodulin lobe occurs in the nucleoli. The N-terminal lobe of calmodulin does not show significant binding to subnuclear structures although similarly to the C-terminal lobe, it accumulates in the nucleoplasm of wheat germ agglutinin-blocked nuclei suggesting that a facilitated nuclear export mechanism exists for calmodulin.

Introduction

Calmodulin (CaM), a ubiquitous Ca^{2+}-binding protein belonging to the EF-hand homolog family, regulates a whole host of processes within the cytoplasm and nucleus of all eukaryotic cells [1,2]. Within the nucleus, CaM has been found to be involved in RNA synthesis [3], DNA synthesis [4-7] and the function of a number of nuclear enzymes and receptors including the estrogen receptor-α [8,9]. Ca^{2+}/CaM dependent phosphorylation of three nuclear proteins of 50-60 kDa [10], CREB [11] and of rat liver heterogenous nuclear ribonucleoproteins hnRNP A2 and C has previously been reported [12]. A structural role for CaM is demonstrated by the finding that elimination of the nuclear function of Ca^{2+}/CaM causes disruption of nuclear structure [13] and a nuclear scaffold protease activity is Ca^{2+}/CaM modulated [14]. Ca^{2+}/CaM also regulates nuclear entry of numerous proteins involved in cell division and proliferation and has been shown to localize to the mitotic apparatus and be essential for mitotic transitions of early sea urchin embryos [15].

A number of previous studies have shown that upon cell stimulation, CaM translocates from the cytoplasm into the nucleus. Indeed, nuclear translocation of CaM has been proposed to support CREB phosphorylation [16,17] and morphine stimulation induced rapid CaM nuclear translocation that was associated with increased CREB phosphorylation [18]. CaM nuclear accumulation was reported in response to corticotrophin stimulation of adrenal cortex cells suggesting a role for CaM in the regulation of hormone effects on nuclear processes [19]. Ca^{2+}/CaM nuclear translocation was shown to require high frequency Ca^{2+} signals, whereas, brief or low frequency signals did not change free Ca^{2+}/CaM concentration in the nucleus [20]. It has, however, been shown that passive diffusion of CaM into the nucleus in low Ca^{2+} is too slow to serve as a means of signal transduction and that upon Ca^{2+} stimulation, CaM is transported into the nucleus by Ca^{2+}-dependent facilitated transport [21]. Further experiments showed an effect of CaM to increase the permeability of the nuclear pore complex [22].

The C- and N-terminal Ca^{2+} binding lobes of CaM have been proposed to have distinct functional properties in processes of target activation [23]. The C- (CaM_{76-148}) and N-lobe (CaM_{1-80}) CaM mutants have been useful in identifying domain interactions within CaM [24]. It has been previously reported that the C-lobe is in a semi-open conformation in apo conditions, whereas the N-lobe is in a closed conformation and in the presence of Ca^{2+} it opens allowing it to bind to targets [25]. However, it has been found that the separated N- and C-terminal lobes of CaM are sufficient to support yeast cell proliferation [26].

The aim of this work was to investigate the Ca^{2+}-dependent and independent binding of calmodulin (CaM) and the role of its N- and C-terminal lobes to nuclear targets such as nucleoli, chromatin and unidentified nucleoplasmic targets. For this study, CaM, labeled at Lys_{75} [21] by 6-carboxy-X-rhodamine (6ROX-CaM) was used in combination with the nucleic acid stain Hoechst 33258 to determine if CaM localized to the same dsDNA labeled regions within the nucleus. Ca^{2+} binding deficient 6ROX-CaM1234 [21] was also used to determine if CaM is required to be in a Ca^{2+}-bound form to bind to nuclear targets. To investigate the binding to nuclear targets of the C- (CaM_{76-148}) and N-lobe (CaM_{1-80}) CaM mutants [24] in the presence and absence of Ca^{2+}, labeled derivatives of the two lobes were constructed. 6ROX-CaM_{76-148} and fluorescein-labeled FL-CaM_{76-148} were used to investigate the binding characteristics of the C-lobe to nuclear targets, whereas 6ROX-CaM_{1-80} and TA-CaM_{1-80} were used to investigate the binding characteristics of the N-lobe to nuclear targets. TA-CaM_{1-80} was used here as a reporter of Ca^{2+} binding and Ca^{2+}-dependent target binding within the cell.

Materials and Methods

Vectors

For the expression of wild type CaM, the $pAED_4$.WT-CaM vector previously obtained from Dr. S. Marston (Imperial College, London, UK) was used. Ca^{2+} binding deficient mutant CaM termed CaM1234 was made in Dr. J.P. Adelman's laboratory by point mutations and was cloned into pET21b vector by Dr. N.N. Kasri, University of Leuven, Belgium. For the expression of the N-lobe CaM fragment CaM_{1-80} and the C-

lobe CaM fragment CaM_{76-148}, pT7/7.CaM_{1-80}, pT7/7.CaM_{76-148} vectors were kindly provided by Professor M. A. Shea and Dr. B. Sorenson, University of Iowa, USA. Protein expression was carried out in BL21-Gold cells (Stratagene)

Proteins and peptides

Protein purification was carried out as previously described for wild type CaM [21]. CaM_{1-80} and CaM_{76-148} were expressed and purified as described for wild type CaM. The concentration of wild type CaM and CaM1234 was measured at 278 nm (A_{278} 0.18 = 1 mg/mL CaM). CaM_{1-80} and CaM_{76-148} were measured by weight. mTrp peptide and its characterization was carried out as previously described [21].

Fluorescent CaM, CaM_{1-80} and CaM_{76-148} fragments

CaM and CaM1234 were labeled with 6ROX as previously described [21]. CaM_{1-80} and CaM_{76-148} were labeled in the same conditions and purified by HPLC to homogeneity as previously described [21]. Labeled protein was digested by trypsin for mass spectrometric analysis as previously described for wild type CaM labeled with 6ROX and DTAF from Molecular probes and TA-Cl [27]. Maldi-tof mass spectrometry was carried out as previously described [21]. Fluorescently labeled tryptic peptides were sequenced by post-source decay analysis to identify the labeled residue. The CaM_{1-80} fragment was determined to be labeled at Lys_{75} and the CaM_{76-148} fragment was modified by the α–amino group of Met_{76} (data not shown). The fluorescence of FL-CaM_{1-80}, 6-ROX-CaM_{1-80}, TA-CaM_{76-148}, FL-CaM_{76-148} and 6ROX-CaM_{76-148} did not significantly change upon Ca^{2+} and mTrp peptide binding (data not shown). TA-CaM_{1-80} fluorescence was, however, sensitive to both Ca^{2+} and mTrp peptide binding as shown in Figure 7.

Cell culture and stimulation

Cell culture and electroporation were carried out as previously described [21]. HeLa cells were electroporated with fluorescent CaM or CaM mutant in 2 mM EGTA. 2.1 mM Ca^{2+} was added to the extracellular medium and cells were imaged for up to 30 minutes. Fluo-4 was administered as AM ester at 4 μM concentration and the cells were incubated at room temperature for 15 minutes before stimulation. mTrp peptide was

added to the external medium and the cells were incubated for 15 minutes prior to stimulation. Fluorescein-labeled wheat germ agglutinin (FL-WGA, Sigma) was co-electroporated to an estimated final concentration of 20 μg/mL with fluorescent CaM derivatives to test for facilitated nuclear transport processes.

Confocal imaging and image analysis

Cells were imaged on a Leica SP system with a 63 X 0.9 water immersion lens, using a 568 nm Krypton laser to excite 6ROX-CaM, a 488 nm Argon laser to excite fluo-4 and a 351/365 nm Argon ion UV laser to excite TA-CaM fluorescence. Images were taken at 6 s intervals for 1200 s at 22 ^{o}C in electroporation buffer and had a box size of 512 X 512 pixels. Image analysis is presented using intensities in representative areas as shown in the figures. The presented single values are within 10% of the mean values obtained by comparing 3-5 areas of interest (not shown).

Statistics

Results are expressed as mean ± s.e.m. (standard error of the mean) and n = number of experiments. All statistical analysis was performed using the parametric test ANOVA-one way. Significant difference was accepted at $P<0.01$.

Results

6ROX-CaM binding to nuclear targets

We have previously reported two properties of CaM regarding its nuclear entry; firstly, we showed Ca^{2+}-dependent and independent entry to the nucleus upon cell stimulation [21] and secondly, we showed that upon robust Ca^{2+} stimulation of the cell, CaM within minutes of stimulation, induces an increase in the permeability of the nuclear pore complex [22]. Here we investigate which structures within the nucleus of HeLa cells, CaM becomes associated with upon its Ca^{2+}-stimulated entry into the nucleus. This is important as these sites may represent the sites of downstream activities of nuclear CaM.

6ROX-CaM nuclear entry was stimulated by the addition of 2.1 mM Ca^{2+} to HeLa cells [21]. As seen in Figure 1, an immediate rise in [Ca^{2+}] was followed by CaM translocation into the nucleus and by association of 6ROX-CaM with the nucleoli. Nucleolic association of CaM occurred with a $t_{1/2}$ of 73 ± 6 s (n = 12). The nucleolic to cytoplasmic fluorescence ratio of 6ROX-CaM significantly increased from 0.92 ± 0.04 to 2.8 ± 0.2. Over the course of the experiment, typically, after 486 ± 43 s the fluorescence intensity of 6ROX-CaM in the nucleoplasm became lower than that associated with other nuclear targets and the nuclear membrane. The nucleoplasmic-cytoplasmic ratio of 6ROX-CaM fluorescence was 1.63 ± 0.05 at its peak, after 317 ± 25 s. However, by 1200 s this had decreased to 1.38 ± 0.12 reflecting the binding of nucleoplasmic 6ROX-CaM to other nuclear targets. An example of the time course of binding to nuclear targets and to the nuclear membrane is shown in Figure 1 suggesting that the structures CaM becomes associated with in the nucleus following Ca^{2+} stimulation, in addition to nucleoli and the nuclear membrane, may be chromatin.

6ROX-CaM co-localization with Hoechst dye

The association of CaM with chromatin has been previously reported [28]. Using the Hoechst dye, we checked whether nuclear CaM and DNA co-localize in HeLa cells. In 2 mM EGTA, before 2.1 mM Ca^{2+} stimulation (see panels at t_0 in Figure 2), 6ROX-CaM showed no co-localization with the Hoechst dye, indicating that CaM did not bind to nucleic acid containing structures in the absence the Ca^{2+}. However, over several minutes after stimulation by extracellular Ca^{2+} addition (513 ± 31 s (n = 3)), 6ROX-CaM fluorescence intensity in the nucleoplasm became lower than that in areas stained by the Hoechst dye, indicating that it was binding to chromatin. However, the Hoechst dye did not appear to co-localize with 6ROX-CaM at the nucleoli (Figure 2).

6ROX-CaM1234 binding to nuclear targets

To determine the role of Ca^{2+} stimulation and if Ca^{2+}/CaM was required for the binding to nuclear targets we electroporated HeLa cells with the Ca^{2+}-non-binding probe 6ROX-CaM1234. The localization of 6ROX-CaM1234 to nuclear targets was analyzed to determine if the binding to nucleoli and chromatin required Ca^{2+}-bound CaM or required

Ca^{2+} to alter the conformation of nuclear targets allowing CaM to bind in a Ca^{2+}-independent form.

Upon stimulation with 2.1 mM Ca^{2+} no initial translocation into the nucleus was seen with the 6ROX-CaM1234 consistent with the fact that Ca^{2+}-dependent facilitated CaM translocation could not take place if Ca^{2+} binding to CaM was inhibited [21]. However, 6ROX-CaM1234 induced an increase in the permeability of the nuclear pores and entered the nucleus with a few minutes delay, as previously described [22]. Typically after 425 ± 65 s (n = 8) there was a slow association with a $t_{1/2}$ of 268 ± 27 s of the 6ROX-CaM1234 in the nucleus with chromatin and the nuclear membrane. Although the fluorescence intensity of 6ROX-CaM1234 in the nucleoli and chromatin did not appear as a large increase, in the nucleoli it was a 2.9 ± 0.5-fold higher compared to the cytoplasm, and 2.3 ± 0.3-fold greater in the nuclear membrane than in the nucleoplasm. This indicated an association of CaM1234 with the subnuclear structures, similarl to that observed with wild type CaM. An example of Ca^{2+}-induced 6ROX-CaM1234 nuclear localization is presented in Figure 3. This indicated that Ca^{2+} was causing a conformational change in these nuclear targets allowing CaM to bind rather than Ca^{2+} causing a conformational change in CaM allowing it to bind.

To totally confirm that the late nuclear binding was due to Ca^{2+} induced changes of these nuclear targets rather than to Ca^{2+} binding to CaM and then allowing it to bind to targets, 10 μM of mTrp peptide was added to the cells after they were electroporated with 6ROX-CaM1234. As shown in Figure 4, it was found that the nuclear entry of 6ROX-CaM1234 in the presence of the mTrp peptide occurred more slowly. The presence of the mTrp peptide did, however, not prevent the binding of 6ROX-CaM1234 to the nuclear targets, firstly confirming that the mTrp peptide can only bind to Ca^{2+}-CaM and that the binding of CaM to chromatin and the nuclear membrane and to some extent to nucleoli, was driven by Ca^{2+} induced changes allowing CaM to bind independently of Ca^{2+}.

Nuclear localization and activation of fluorescently labeled C- and N-lobe CaM mutants

The role of the individual C-and N-terminal lobes of CaM in subnuclear targeting was tested by using fluorescently labeled CaM fragments corresponding to residues 76-

148 and 1-80 representing the C- and N-lobes of CaM, respectively. CaM_{76-148} and CaM_{1-80} were labeled with fluorophores to report localization and and/or activation by Ca^{2+} and target binding and were introduced into HeLa cells by electroporation. The associations with unidentified nuclear targets, nucleoli, chromatin and the nuclear membrane of 6ROX-CaM_{76-148} or FL-CaM_{76-148}, representing the C-lobe, and 6ROX-CaM_{1-80} or TA-CaM_{1-80}, representing the N-lobe, were analyzed in low Ca^{2+} and in a Ca^{2+} stimulated state and compared to the binding of full length CaM in similar conditions. The mTrp peptide was added to the cells to determine if the inhibitor would prevent CaM_{76-148} or CaM_{1-80} binding.

Nuclear target binding of CaM_{76-148} in low [Ca^{2+}]

HeLa cells were electroporated with either FL-CaM_{76-148} or 6ROX-CaM_{76-148} in 2 mM EGTA to analyze C-lobe binding in low Ca^{2+} conditions. As seen in the example shown in Figure 5A, 6ROX-CaM_{76-148} accumulated in the nucleus of unstimulated cells. Upon analysis it was found that for 6ROX-CaM_{76-148} in 2 mM EGTA, the nucleoplasmic to cytoplasmic ratio was 1.95 ± 0.49, the nucleolic to cytoplasmic ratio was 2.41 ± 0.97 and the nuclear membrane to cytoplasmic ratio was 1.61 ± 0.42 (n = 7). For FL-CaM_{76-148}, the nucleoplasmic to cytoplasmic ratio of was found to be 1.9 ± 0.43, the nucleolic to cytoplasmic ratio was 2.52 ± 0.93 and the nuclear membrane to cytoplasmic ratio was 1.86 ± 0.45 (n = 7) (Figure 8 illustrates such an example). The values for the CaM_{76-148} fragment thus were significantly different from the values found for 6ROX-CaM in 2 mM EGTA which had a nucleoplasmic to cytoplasmic ratio of 1.18 ± 0.03 and a nucleolic to cytoplasmic ratio = 0.92 ± 0.04 (n = 19). Thus, both FL-CaM_{76-148} and 6ROX-CaM_{76-148} were bound to nucleoli, chromatin and the nuclear membrane before Ca^{2+} stimulation unlike full-length fluorescently labeled CaM. A possible explanation for this phenomenon may be that due to its small size, the CaM_{76-148} fragment unlike full length CaM does not require Ca^{2+}-dependent facilitated transport but enters the nucleus by diffusion and it becomes trapped there. This may occur due to high affinity binding to nuclear components and/or by impairment of a nuclear export system which requires full length CaM for functioning.

Nuclear target binding of CaM_{76-148} in high intracellular [Ca^{2+}]

Upon cell stimulation with 2.1 mM Ca^{2+} no significant nuclear translocation of either 6ROX-CaM_{76-148} (Figure 5) or FL-CaM_{76-148} (Figure 8B) was observed. However, the C-lobe CaM from the nucleoplasm demonstrated further rapid binding to the nucleoli, nuclear membrane and chromatin with a $t_{1/2}$ of 25 ± 4.1 for 6ROX-CaM_{76-148} (n = 4) and 35 ± 5.4 for FL-CaM_{76-148} (n = 4). The nucleolic to nucleoplasm ratio significantly increased from 1.2 ± 0.06 to 3.3 ± 0.17 (6ROX-CaM_{76-148}) and from 1.3 ± 0.08 to 3.87 ± 0.33 (FL-CaM_{76-148}). The nuclear membrane to nucleoplasm ratio also significantly increased from 0.82 ± 0.02 to 1.92 ± 0.19 (FL-CaM_{76-148}) and from 0.98 ± 0.03 to 1.97 ± 0.1 (6ROX-CaM_{76-148}). Thus, C-lobe CaM demonstrated a similar response to full length CaM upon Ca^{2+} stimulation.

Nuclear target binding of CaM_{76-148} inhibited by mTrp peptide

We checked the specificity of the C-lobe CaM nuclear binding by using the CaM inhibitor mTrp peptide. The application of 10 μM mTrp peptide to HeLa cells loaded with 6ROX-CaM_{76-148} in 2 mM EGTA and then stimulated with 2.1 mM Ca^{2+} largely prevented binding to nuclear targets and 6ROX-CaM_{76-148} remained distributed in the nucleoplasm (n = 3) (Figure 6). These data show that the association of 6ROX-CaM_{76-148} with nuclear targets seen above was specific to CaM rather than representing trapping in subnuclear structures.

Lack of nuclear target binding of CaM_{1-80} in low [Ca^{2+}]

HeLa cells were electroporated with 6ROX-CaM_{1-80} in 2 mM EGTA to analyse N-lobe nuclear binding in low Ca^{2+} conditions. Upon analysis it was found that 6ROX-CaM_{1-80}, unlike 6ROX-CaM_{76-148}, was not bound to nucleoli, chromatin or the nuclear membrane before Ca^{2+} stimulation. The nucleoplasmic to cytoplasmic ratio of 6ROX-CaM_{1-80} was found to be 1.39 ± 0.04 (n = 9) and the nucleolic to cytoplasmic ratio was 0.99 ± 0.04 (Figure 7). This was significantly different from the nucleoplasmic to cytoplasmic ratio of 1.95 ± 0.49 and the nucleolic to cytoplasmic ratio of 2.41 ± 0.97 found with 6ROX-CaM_{76-148} in the same conditions. This indicated that the C-lobe of CaM was able to bind to nuclear targets with a higher affinity than the N-lobe. However

Biochemical Journal Immediate Publication. Published on 16 Oct 2006 as manuscript BJ20061111

the nucleoplasmic to cytoplasmic ratio of 6ROX-CaM_{1-80} was still significantly higher than 6ROX-CaM (1.39 ± 0.04 compared to 1.18 ± 0.03, $p < 0.001$). It is noteworthy that in contrast with C-lobe, neither the N-lobe nor full length CaM was able to bind to nucleoli, chromatin or the nuclear membrane in the absence of Ca^{2+}.

Lack of nuclear target binding of CaM_{1-80} in high [Ca^{2+}]

Upon cell stimulation with 2.1 mM Ca^{2+} no further significant nuclear translocation of fluorescently-labeled CaM_{1-80} was observed. In comparison to the C-lobe, no significant binding of the N-lobe to nucleoli, chromatin or the nuclear membrane was found and 6ROX-CaM_{1-80} remained in the nucleoplasm. After 500 s, the nucleoplasmic to cytoplasm ratio was 1.4 ± 0.05 showing no significant increase and the nucleolic to nucleoplasmic ratio slightly increased, but not significantly, from 0.72 ± 0.03 to 0.79 ± 0.06 (Figure 7). This suggested that either the N-lobe CaM was unable to bind to nucleoli, chromatin and the nuclear membrane or it had a lower affinity for either Ca^{2+} or target binding than endogenous full length CaM.

Ca^{2+} activation of TA-CaM_{1-80} activation upon stimulation

To check that CaM_{1-80} was binding to Ca^{2+}, HeLa cells were electroporated with TA-CaM_{1-80} in 2 mM EGTA and stimulated with 2.1 mM Ca^{2+}. Upon cell stimulation there was a 1.88 ± 0.12 (n = 13) fold increase in the nucleoplasmic fluorescence indicating that TA-CaM_{1-80} was binding to Ca^{2+} and possibly to unidentified nucleoplasmic proteins. There was also a 2.89 ± 0.12 fold increase in the nucleolar fluorescence indicating Ca^{2+} binding and some nucleolar accumulation of TA-CaM_{1-80} (Figure 8A).

Simultaneous imaging of C- and N-CaM domains in the same cell

FL-CaM_{76-148} and TA-CaM_{1-80} were electroporated into the same cells to directly compare the binding differences between the N and C-domains. Upon Ca^{2+} stimulation, FL-CaM_{76-148} immediately bound to nucleoli, chromatin and the nuclear membrane as seen for 6ROX-CaM_{76-148} (Figure 4), whereas TA-CaM_{1-80} showed very little binding to these targets but demonstrated typical nucleoplasmic and nucleolar increases in

fluorescence (n = 4) (Figure 8A-D). In Figure 8D, due to a large reduction in fluorescence of FL-CaM_{76-148} that occurred upon Ca^{2+} stimulation likely as a result of a decrease in pH, fluorescence intensities measured in nuclear regions were related to that in cytoplasm in each frame. Solution fluorescence measurements showed that the fluorescence of TA-CaM_{1-80} increased 1.9-fold upon Ca^{2+} binding giving an apparent dissociation constant K_d for Ca^{2+} of 3.85 ± 1.2 μM (Figure 8E) and the addition of Trp peptide up to 600 nM increased the fluorescence a further 2.7-fold in these Ca^{2+} saturated conditions (Figure 8F). A K_d value of 208 ± 26 nM was measured for mTrp peptide binding to TA-CaM_{1-80}. However, in the absence of Ca^{2+} the fluorescence of TA-CaM_{1-80} only increased 1.2-fold upon additions of mTrp peptide up to 500 nM. This suggested that CaM_{1-80} needed to be in an open conformation induced by Ca^{2+} binding to be able to bind to the mTrp peptide.

Mechanism of nuclear accumulation of C- and N-CaM domains in resting HeLa cells

In order to determine if the inhibition of facilitated transport would prevent nuclear entry of the C and N-domains as was seen in cells electroporated with full length 6ROX-CaM [35], FL-WGA (estimated final concentration 20 μg/mL) was co-electroporated into HeLa cells with either 6ROX-CaM_{76-148} or 6ROX-CaM_{1-80} in 2 mM EGTA. FL-WGA was found to permeate both the plasma and the nuclear membrane in a subsection of electroporated cells (Figure 9A and C), but in a different subsection of cells, FL-WGA presented only in the plasma membrane but not in the nuclear membrane (Figure 9B and D). Surprisingly, upon visualization of C-domain CaM, it was found that cells containing the FL-WGA inhibitor associated with the nuclear membrane showed 6ROX-CaM_{76-148} concentrated in the nucleus with none in the cytoplasm (Figure 9A). In cells that also contained FL-WGA but only in the plasma membrane and not in the nuclear membrane, 6ROX-CaM_{76-148} was distributed in the normal way (Figure 9B). A similar pattern was seen with 6ROX-CaM_{1-80}, again in the presence of FL-WGA inhibiting facilitated transport, the N-lobe was concentrated in the nucleus with none present in the cytoplasm (Figure 9C). Cells that did not have the association of FL-WGA with the nuclear membrane showed normal distribution of 6ROX-CaM_{1-80} (Figure 9D). This was the complete opposite of what was found in cells containing 6ROX-CaM and

FL-WGA [21]. In those cells 6ROX-CaM nuclear entry was blocked whereas here 6ROX-CaM_{76-148} and 6ROXCaM_{1-80} were both prevented from exiting the nucleus.

Discussion

CaM has been reported to be localized to the nucleoli, non-peripheral chromatin and peripheral chromatin associated with the nuclear membrane [29]. Here 6ROX-CaM in low Ca^{2+} conditions was found to be 1.2-fold higher in the nucleoplasm of HeLa cells compared to the cytoplasm. However, no binding to nucleoli, chromatin or the nuclear membrane was detected in these conditions. Upon Ca^{2+} stimulation 6ROX-CaM immediately bound to nucleoli and translocation from the cytoplasm to the nucleus was observed. Typically 7 – 9 minutes later, 6ROX-CaM began to associate with other structures and cells loaded with the nucleic acid stain Hoechst dye and 6ROX-CaM suggested that these structures were chromatin.

6ROX-CaM1234 similarly showed no association with nucleoli, chromatin and the nuclear membrane before addition with Ca^{2+} and as expected no immediate binding to the nucleoli was seen upon cell stimulation. However, 6ROX-CaM1234 also showed late binding to chromatin and the nuclear membrane minutes after stimulation. This suggested that Ca^{2+} was inducing a conformational change in these nuclear targets allowing CaM to bind rather than Ca^{2+} inducing a change on CaM allowing it to bind. This is indeed possible; an interaction of Ca^{2+} with chromatin material has been reported in sympathetic neuronal cells [30]. It was also shown in vitro that Ca^{2+} and ATP induced structural changes on the histone H1, a major constituent of chromatin that contributes to chromatin condensation [31]. It is possible therefore that Ca^{2+}-induced chromatin changes were allowing CaM or a CaM-binding protein to bind to chromatin. Indeed, it has been found that a 62 kDa CaM-binding protein, p62, which has a low-affinity for CaM, was localized over condensed chromatin and the nuclear matrix in quiescent astrocytes, hepatocytes and cortical astroglia cells [32]. Here, the results suggest that 6ROX-CaM or 6ROX-CaM1234 may not have bound to chromatin directly but was bound to a CaM-binding protein independently of Ca^{2+}. The conformational change on chromatin induced by Ca^{2+} then allowed CaM to associate via a CaM-binding protein.

The binding of the N and C-lobe CaM fragments to nucleoli, chromatin and the nuclear membrane were also investigated in HeLa cells. The C-lobe is in a semi-open conformation in apo conditions, whereas the N-lobe is in a closed conformation and in the presence of Ca^{2+} it opens allowing it to bind to targets [25]. It has been found that Ca^{2+} binding sites III and IV in the C-lobe have a 10-fold higher affinity for Ca^{2+} than sites I and II in the N-lobe [24,33]. However, the isolated N-lobe has a higher Ca^{2+} affinity than when part of the full length CaM indicating that Ca^{2+} binding to sites I and II is of a lower affinity in the presence of the C-lobe [24]. Previous studies have also shown that C-domain was able to bind to NR1 C0 [34] and melittin [35] in apo conditions, whereas the N-domain only became associated in Ca^{2+} conditions.

The ability of apo-$CaM_{76\text{-}148}$ to bind to nuclear targets was seen here with both 6ROX-$CaM_{76\text{-}148}$ and FL-$CaM_{76\text{-}148}$ demonstrating binding to nucleoli, chromatin and the nuclear membrane in low Ca^{2+} conditions. This contrasted with the finding that full length CaM did not bind to nucleoli, chromatin or the nuclear membrane in the absence of Ca^{2+}. It was also observed that the C-lobe was 1.9-fold higher in the nucleoplasm compared to the cytoplasm indicating that the C-lobe bound unidentified nucleoplasmic proteins in apo conditions. In contrast with the similarly sized 9.5 kDa FL-dextran, which only showed a ratio of 0.92 as it remained unbound in the nucleus [21], $CaM_{76\text{-}148}$ was able to bind to nucleoplasmic targets, nucleoli, chromatin and the nuclear membrane therefore keeping it at a higher concentration the nucleus. Upon the addition of Ca^{2+} both 6ROX-$CaM_{76\text{-}148}$ and FL-$CaM_{76\text{-}148}$ from the nucleoplasm were seen to further bind to nucleoli, chromatin and the nuclear membrane with $t_{1/2}$ values of 25 s and 35 s, respectively. This was significantly faster than the binding of full-length 6ROX-CaM to nucleoli which occurred with a $t_{1/2}$ of 72 s consistent with the C-lobe having a higher affinity for nucleolar CaM binding proteins and a smaller size than full-length CaM. Another interesting difference was the lack of delay of C-lobe CaM to bind to chromatin and the nuclear membrane whereas full length CaM typically did not bind to these targets until 8 minutes post stimulation. If the theory presented here that chromatin undergoes a conformational change before CaM can bind is correct then the same restrictions might not apply to the C-lobe CaM. A pool of FL-$CaM_{76\text{-}148}$ and 6ROX-$CaM_{76\text{-}148}$ must have been bound to unidentified targets in the nucleoplasm in low free Ca^{2+} otherwise apo-$CaM_{76\text{-}148}$ would have all bound to nucleoli, chromatin and the nuclear membrane. Upon

Ca^{2+} stimulation it was possible that this pool of bound CaM_{76-148} in the nucleoplasm was released and became free to bind with nucleoli, chromatin and the nuclear membrane. Indeed it has been reported that only 5 % of CaM was free in Ca^{2+}-independent conditions and upon Ca^{2+} stimulation a large pool of this CaM was released [36].

6ROX-CaM_{1-80} showed a nucleoplasmic to cytoplasmic ratio of 1.4 in low Ca^{2+} conditions, which was still significantly higher than the ratio of 0.92 for 6ROX-CaM. This indicated that the N-lobe was able to bind to nucleoplasmic targets in the absence of Ca^{2+} which was surprising due to the closed conformation of the N-domain in apo conditions preventing it from binding to targets. However, certain targets appear to bind to the N-domain in the absence of Ca^{2+} even though it is in a closed conformation, for example, the ryanodine receptor RYR1 [36] and voltage-gated Ca^{2+} channels [37]. The nucleoplasmic to cytoplasmic ratio was still found to be lower compared to the C-lobe (1.4 compared to 1.9) indicating that the C-lobe had a higher affinity for nucleoplasmic targets.

Upon Ca^{2+} stimulation, there was no significant increase in the binding of 6ROX-CaM_{1-80} to nucleoli, chromatin or the nuclear membrane, indicating two possibilities. Firstly, it was possible that the N-domain could not bind to the nucleolar and chromatin CaM-binding proteins in the absence of a C-domain. A second possibility was that these targets had a lower affinity for Ca^{2+}-CaM_{1-80} than for endogenous full length CaM. As seen in Figure 7F, Trp peptide had a 6 x 10^4-fold lower affinity for Ca^{2+}/TA-CaM_{1-80} than for Ca^{2+}/CaM [27]. The 2-fold increase in fluorescence of TA-CaM_{1-80} indicated that it was binding to Ca^{2+} causing the N-lobe to enter an open conformation. Therefore it is more than likely that endogenous Ca^{2+}-CaM competed out the binding of the N-lobe. Similarly in cells electroporated with both FL-CaM_{76-148} and TA-CaM_{1-80} only the C-lobe was seen to bind to nucleoli and chromatin with very limited binding of the N-lobe. Again this demonstrated that the C-lobe had a higher affinity for these targets than the N-lobe.

Upon the co-electroporation of 6ROX-CaM_{76-148} or 6ROX-CaM_{1-80} with WGA, both lobes were unexpectedly trapped in the nucleus and over a period of 30 minutes no diffusion back into the cytoplasm of either CaM lobe was seen. This was the complete opposite of what was seen with 6ROX-CaM or 6ROX-CaM1234 in apo conditions, where in the presence of WGA, they were significantly more cytoplasmic [21]. It is

known that WGA only prevents facilitated transport, import as well as export, but not passive diffusion [38], therefore, the observations suggest that both C and N-lobes of CaM are in a bound state in the nucleus otherwise both would diffuse back into the cytoplasm. One obvious question is why neither lobe is distributed similarly in the absence of WGA i.e. all in the nucleus. The possible answer to this is that upon electroporation both lobes of CaM are able to diffuse into the nucleus attracted to nucleoplasmic targets and nucleoli and chromatin in the case of CaM_{76-148}. Once there they bind to these nuclear targets in the absence of Ca^{2+}. These nucleoplasmic targets that either lobe binds to in the absence of Ca^{2+} could be shuttling proteins that shuttle continuously between the nucleus and cytoplasm and contain import and export sequences. Therefore in the presence of WGA they might become trapped in the nucleus due to the inhibition of facilitated transport. One such protein family could be the heterogeneous nuclear RNA-binding proteins (hnRNP proteins) [39]. Full-length CaM, however, does not show the same properties as the two separate lobes. Upon electroporation CaM is too large to pass through the nuclear pores in the absence of Ca^{2+} and import into the nucleus requires it to associate with a CaM-binding protein with an NLS sequence. In the presence of WGA this complex cannot be taken up into the nucleus due the inhibition of facilitated transport.

Therefore, in conclusion it is shown that CaM and CaM1234 can bind to chromatin upon Ca^{2+} stimulation due to a conformational change induced by Ca^{2+} on chromatin rather than a conformational change on CaM. Both the C and N-lobes of CaM appear to be able to associate with nucleoplasmic targets in apo conditions, as indicated by higher nucleoplasmic to cytoplasmic ratios than full-length CaM and by the observation that both domains are trapped in the nucleus in the presence of WGA. The C terminal lobe of CaM, CaM_{76-148} is also able to bind to chromatin and nucleoli in apo conditions but the N terminal lobe, CaM_{1-80} does not show any association and is competed out upon Ca^{2+} stimulation due to its lower affinity for targets than full-length endogeous CaM.

Acknowledgement: This work was supported by the Medical Research Council, UK.

References

[1] Bachs, O., Agell, N. and Carafoli, E. (1994) Calmodulin and calmodulin-binding proteins in the nucleus. Cell Calcium **16**, 289-296.

[2] Persechini, A., Moncrief, N. D. and Kretsinger, R. H. (1989) The EF-hand family of calcium modulated proteins. Trends in Neurosci. **12**, 462-467.

[3] Pardo,J.P. & Fernandez,F. (1982) Effect of calcium and calmodulin on RNA synthesis in isolated nuclei from rat liver cells. FEBS Lett**. 143,** 157-160.

[4] Wang,J., Moreira,K.M., Campos,B., Kaetzel,M.A., & Dedman,J.R. (1996) Targeted neutralization of calmodulin in the nucleus blocks DNA synthesis and cell cycle progression. Biochim. Biophys. Acta **1313,** 223-228.

[5] King,K.L., Moreira,K.M., Babcock,G.F., Wang,J., Campos,B., Kaetzel,M.A., & Dedman,J.R. (1998) Temporal inhibition of calmodulin in the nucleus. Biochim. Biophys. Acta **1448,** 245-253.

[6] Subramanyam,C., Honn,S.C., Reed,W.C., & Reddy,G.P. (1990) Nuclear localization of 68 kDa calmodulin-binding protein is associated with the onset of DNA replication. J. Cell Physiol. **144,** 423-428.

[7] Reddy,G.P., Reed,W.C., Deacon,D.H., & Quesenberry,P.J. (1994) Growth factor modulated calmodulin-binding protein stimulates nuclear DNA synthesis in hemopoietic progenitor cells. Biochemistry **33,** 6605-6610.

[8] Bouhoute,A. & Leclercq,G. (1995) Modulation of estradiol and DNA binding to estrogen receptor upon association with calmodulin. Biochem. Biophys. Res. Commun. **208,** 748-755.

[9] Li,L., Li,Z., & Sacks,D.B. (2005) The transcriptional activity of estrogen receptor-alpha is dependent on Ca^{2+}/calmodulin. J. Biol. Chem. **280,** 13097-13104.

[10] Maizels,E.T. & Jungmann,R.A. (1983) Ca^{2+}-calmodulin-dependent phosphorylation of soluble and nuclear proteins in the rat ovary. Endocrinology **112,** 1895-1902.

[11] Sheng,M., Thompson,M.A., & Greenberg,M.E. (1991) CREB: a Ca^{2+}-regulated transcription factor phosphorylated by calmodulin-dependent kinases. Science **252,** 1427-1430.

[12] Bosser,R., Faura,M., Serratosa,J., Renau-Piqueras,J., Pruschy,M., & Bachs,O. (1995) Phosphorylation of rat liver heterogeneous nuclear ribonucleoproteins A2 and C can be modulated by calmodulin. Mol. Cell Biol. **15,** 661-670.

[13] Wang,J., Campos,B., Jamieson,G.A., Jr., Kaetzel,M.A., & Dedman,J.R. (1995) Functional elimination of calmodulin within the nucleus by targeted expression of an inhibitor peptide. J. Biol. Chem. **270,** 30245-30248.

[14] Madsen,K.R., Fiskum,G., & Clawson,G.A. (1990) Regulation of nuclear scaffold protease activity by calcium. Exp. Cell Res. **187,** 343-345.

[15] Török,K., Wilding,M., Groigno,L., Patel,R., & Whitaker,M. (1998) Imaging the spatial dynamics of calmodulin activation during mitosis. Curr. Biol. **8,** 692-699.

[16] Deisseroth,K., Bito,H., & Tsien,R.W. (1996) Signaling from synapse to nucleus: postsynaptic CREB phosphorylation during multiple forms of hippocampal synaptic plasticity. Neuron **16,** 89-101.

[17] Mermelstein,P.G., Deisseroth,K., Dasgupta,N., Isaksen,A.L., & Tsien,R.W. (2001) Calmodulin priming: nuclear translocation of a calmodulin complex and the memory of prior neuronal activity. Proc. Natl. Acad. Sci. U. S. A. **98,** 15342-15347.

[18] Wang,D., Tolbert,L.M., Carlson,K.W., & Sadee,W. (2000) Nuclear Ca^{2+}/calmodulin translocation activated by mu-opioid (OP3) receptor. J. Neurochem. **74,** 1418-1425.

[19] Harper,J.F., Cheung,W.Y., Wallace,R.W., Huang,H.L., Levine,S.N., & Steiner,A.L. (1980) Localization of calmodulin in rat tissues. Proc. Natl. Acad. Sci. U. S. A. **77,** 366-370.

[20] Teruel,M.N., Chen,W., Persechini,A., & Meyer,T. (2000) Differential codes for free Ca(2+)-calmodulin signals in nucleus and cytosol. Curr. Biol. **10,** 86-94.

[21] Thorogate,R. & Török,K. (2004) Ca^{2+}-dependent and -independent mechanisms of calmodulin nuclear translocation. J. Cell Sci. **117,** 5923-5936.

[22] Thorogate,R. & Török,K. (2006) Nuclear pore gating by calmodulin. Calcium Binding Proteins **1,** 36-44.

[23] Vetter,S.W. & Leclerc,E. (2003) Novel aspects of calmodulin target recognition and activation. Eur. J. Biochem. **270,** 404-414.

[24] Sorensen,B.R. & Shea,M.A. (1998) Interactions between domains of apo calmodulin alter calcium binding and stability. Biochemistry **37,** 4244-4253.

[25] Swindells,M.B. & Ikura,M. (1996) Pre-formation of the semi-open conformation by the apo-calmodulin C-terminal domain and implications binding IQ-motifs. Nat. Struct. Biol. **3,** 501-504.

[26] Sun,G.H., Ohya,Y., & Anraku,Y. (1991) Half-calmodulin is sufficient for cell proliferation. Expressions of N- and C-terminal halves of calmodulin in the yeast Saccharomyces cerevisiae. J. Biol. Chem. **266,** 7008-7015.

[27] Török,K. & Trentham,D.R. (1994) Mechanism of 2-chloro-(epsilon-amino-Lys75)-[6-[4-(N,N- diethylamino)phenyl]-1,3,5-triazin-4-yl]calmodulin interactions with smooth muscle myosin light chain kinase and derived peptides. Biochemistry **33,** 12807-12820.

[28] Iwasa,Y., Iwasa,T., Matsui,K., Higashi,K., & Miyamoto,E. (1981) Interaction of calmodulin with chromatin associated proteins and myelin basic protein. Life Sci. **29,** 1369-1377.

[29] Wong,E.C., Saffitz,J.E., & McDonald,J.M. (1991) Association of calmodulin with isolated nuclei from rat hepatocytes. Biochem. Biophys. Res. Commun. **181,** 1548-1556.

[30] Przywara,D.A., Bhave,S.V., Bhave,A., Wakade,T.D., & Wakade,A.R. (1991) Stimulated rise in neuronal calcium is faster and greater in the nucleus than the cytosol. FASEB J. **5,** 217-222.

[31] Tarkka,T., Oikarinen,J., & Grundstrom,T. (1997) Nucleotide and calcium-induced conformational changes in histone H1. FEBS Lett. **406,** 56-60.

[32] Portoles,M., Faura,M., Renau-Piqueras,J., Iborra,F.J., Saez,R., Guerri,C., Serratosa,J., Rius,E., & Bachs,O. (1994) Nuclear calmodulin/62 kDa calmodulin-binding protein complexes in interphasic and mitotic cells. J. Cell Sci. **107 (Pt 12),** 3601-3614.

[33] VanScyoc,W.S., Sorensen,B.R., Rusinova,E., Laws,W.R., Ross,J.B., & Shea,M.A. (2002) Calcium binding to calmodulin mutants monitored by domain-specific intrinsic phenylalanine and tyrosine fluorescence. Biophys. J. **83,** 2767-2780.

[34] Akyol,Z., Bartos,J.A., Merrill,M.A., Faga,L.A., Jaren,O.R., Shea,M.A., & Hell,J.W. (2004) Apo-calmodulin binds with its C-terminal domain to the N-methyl-D-aspartate receptor NR1 C0 region. J. Biol. Chem. **279,** 2166-2175.

[35] Sorensen,B.R., Eppel,J.T., & Shea,M.A. (2001) Paramecium calmodulin mutants defective in ion channel regulation associate with melittin in the absence of calcium but require it for tertiary collapse. Biochemistry **40,** 896-903.

[36] Luby-Phelps,K., Hori,M., Phelps,J.M., & Won,D. (1995) Ca(2+)-regulated dynamic compartmentalization of calmodulin in living smooth muscle cells. J. Biol. Chem. **270,** 21532-21538.

[37] Zhang,H., Zhang,J.Z., Danila,C.I., & Hamilton,S.L. (2003) A noncontiguous, intersubunit binding site for calmodulin on the skeletal muscle Ca^{2+} release channel. J. Biol. Chem. **278,** 8348-8355.

[38] Middeler,G., Zerf,K., Jenovai,S., Thulig,A., Tschodrich-Rotter,M., Kubitscheck,U., & Peters,R. (1997) The tumor suppressor p53 is subject to both nuclear import and export, and both are fast, energy-dependent and lectin-inhibited. Oncogene **14,** 1407-1417.

[39] Vautier,D., Chesne,P., Cunha,C., Calado,A., Renard,J.P., & Carmo-Fonseca,M. (2001) Transcription-dependent nucleocytoplasmic distribution of hnRNP A1 protein in early mouse embryos. J. Cell Sci. **114,** 1521-1531.

[40] Tzortzopoulos,A., Best,S.L., Kalamida,D., & Török,K. (2004) Ca^{2+}/calmodulin-dependent activation and inactivation mechanisms of alphaCaMKII and phospho-Thr286-alphaCaMKII. Biochemistry **43,** 6270-6280.

Figure 1: 6ROX-CaM binding to nuclear targets after stimulation. A) HeLa cell electroporated with 6ROX-CaM in 2 mM EGTA (t_0) and stimulated with 2.1 mM Ca^{2+} (t_{43}). In the example shown, 6ROX-CaM bound to nucleoli upon stimulation with a $t_{1/2}$ of 92 s and the fluorescence intensity in the nucleolus relative to the cytoplasm increased 2.91-fold. As seen in the image taken at t_{601} and onwards, redistribution of 6ROX-CaM from the nucleoplasm to other nuclear targets and the nuclear membrane became pronounced. Intensity measurements were made in single windows selected in representative areas. Time course of **(B)** 6ROX-CaM nuclear translocation and **(C)** the Ca^{2+} transient indicated by fluo-4 over 1200 s are shown in the (♦, orange) nucleolus, (▲, blue) nucleoplasm, (■, mauve) nuclear membrane and the (*, green) cytoplasm. It is noteworthy that the time courses of Ca^{2+} decay in this experiment and those shown in Figure 4C, 5C were slower to decay with $t_{1/2}$-s of > 400 s than those presented in Figures 6D and 7D which had a $t_{1/2}$ of decay of ~ 200 s. We have not identified any significant difference between the CaM cellular redistribution patterns and time courses as a result of difference in the Ca^{2+} sequestration time courses. Arrow indicates 2.1 mM Ca^{2+} addition.

Figure 2: 6ROX-CaM and Hoechst nuclear localization upon stimulation. HeLa cell loaded with **A)** 6ROX-CaM, **B)** Hoechst dye and **C**) overlay of 6ROX-CaM and Hoechst images. Cells were stimulated with 2.1 mM Ca^{2+}. Upon Ca^{2+} stimulation, 6ROX-CaM bound immediately to the nucleoli with a $t_{1/2}$ of 75 s and then showed a second slower binding step at t_{500} where it became localized with the Hoechst dye, indicating that it was possibly binding to chromatin (t_{900}).

Figure 3: 6ROX-CaM1234 binding to nuclear targets after Ca^{2+} stimulation. A) HeLa cell electroporated with 6ROX-CaM1234 and fluo-4 in 2 mM EGTA and stimulated with 2.1 mM Ca^{2+} (t_{72}). No translocation of 6ROX-CaM1234 was seen unlike 6ROX-CaM upon Ca^{2+} stimulation, however binding to nucleoli, chromatin and the nuclear membrane began at t_{510} and showed a slow association with a $t_{1/2}$ of 314 s. Time course of **(B)** 6ROX-CaM1234 nuclear binding and **(C)** the Ca^{2+} transient measured by fluo-4 over 1800 s in the (♦, orange) nucleolus, (▲, blue) nucleoplasm, (■, mauve)

nuclear membrane and the (*, green) cytoplasm. Arrow indicates 2.1 mM Ca^{2+} addition.

Figure 4: 6ROX-CaM1234 binding to nuclear targets after Ca^{2+} stimulation in the presence of mTrp peptide. A) HeLa cells electroporated with 6ROX-CaM1234 and fluo-4 in 2 mM EGTA, loaded with 10 μM mTrp peptide and stimulated with 2.1 mM Ca^{2+} (t_{130}). Time course of **B)** 6ROX-CaM1234 nuclear binding and **C)** the Ca^{2+} transient measured by fluo-4 in the (♦, orange) nucleolus, (▲, blue) nucleoplasm, (■, mauve) nuclear membrane and the (*, green) cytoplasm. Arrow indicates 2.1 mM Ca^{2+} addition.

Figure 5: 6ROX-CaM_{76-148} nuclear binding upon stimulation. A) HeLa cell was electroporated with 6ROX-CaM_{76-148} in 2 mM EGTA and stimulated with 2.1 mM Ca^{2+}. Most of 6ROX-CaM_{76-148}, which was already present in the nucleus, rapidly accumulated in the nucleoli with a $t_{1/2}$ of 20 s and also bound to chromatin and the nuclear membrane. Time course of **(B)** 6ROX-CaM_{76-148} nuclear binding and **(C)** the Ca^{2+} transient measured by fluo-4 over 400 s in the (♦, orange) nucleolus, (▲, blue) nucleoplasm, (■, mauve) nuclear membrane and the (*, green) cytoplasm. Arrows indicate 2.1 mM Ca^{2+} addition.

Figure 6: 6ROX-CaM_{76-148} nuclear binding inhibited by mTrp peptide. HeLa cell electroporated with **(A)** 6ROX-CaM_{76-148} and **(B)** fluo-4 and loaded with 10 μM mTrp peptide. Cell was stimulated with 2.1 mM Ca^{2+}, however, no additional binding was seen to nuclear targets. Time course of **(C)** 6ROX-CaM_{76-148} nuclear binding and **(D)** the Ca^{2+} transient measured by fluo-4 over 1200 s in the (♦, orange) nucleolus, (▲, blue) nucleoplasm and the (*, green) cytoplasm. Arrow indicates 2.1 mM Ca^{2+} addition.

Figure 7: 6ROX-CaM_{1-80} nuclear binding upon stimulation. HeLa cell was electroporated with **(A)** 6ROX-CaM_{1-80} and **(B)** fluo-4 in 2 mM EGTA and stimulated with 2.1 mM Ca^{2+}. No nuclear translocation was observed and no significant binding to nucleoli, chromatin or the nuclear membrane was seen. Time course of **(C)** 6ROX-CaM_{1-80} nuclear binding and **(D)** the Ca^{2+} transient measured by fluo-4 over 1200 s in the (♦,

orange) nucleolus, (▲, blue) nucleoplasm and the (*, green) cytoplasm. Arrow indicates 2.1 mM Ca^{2+} addition.

Figure 8: TA-CaM_{1-80} and FL-CaM_{76-148} nuclear binding upon stimulation. HeLa cell electroporated with **(A)** TA-CaM_{1-80} and (**B)** FL-CaM_{76-148} in 2 mM EGTA and stimulated with 2.1 mM Ca^{2+}. FL-CaM_{76-148} bound to nucleoli with a $t_{1/2}$ of 15 s and TA-CaM_{1-80} showed a 2.1 and 2.5-fold rise in fluorescence in the nucleoplasm and nucleoli respectively at F_{max}. Time course of **(C)** TA-CaM_{1-80} nuclear binding and **(D)** the fluorescence increase in FL-CaM_{76-148} upon Ca^{2+} and target binding over 400 s in the (♦, orange) nucleolus, (▲, blue) nucleoplasm, (■, mauve) nuclear membrane and the (*, green) cytoplasm. Arrow indicates 2.1 mM Ca^{2+} addition. **(E)** Ca^{2+} titration of TA-CaM_{1-80}. Buffer contained 2 mM EGTA, 100 mM KCl, 2 mM $MgCl_2$ and 50 mM PIPES-K^+, pH 7.0 at 21 ^oC and 30 nM TA-CaM_{1-80}. Free Ca^{2+} concentrations were calculated using a K_d of 4.35 x 10^{-7} M for EGTA determined in similar buffer and ionic strength conditions and calculated [Ca^{2+}] were checked by titration of fluo-3 fluorescence as previously described [40]. Upon Ca^{2+} additions up to 1 mM free Ca^{2+} there was a 1.92-fold fluorescence increase (excitation = 365 nm; emission = 420 nm). Best fit K_d value of 2.75 ± 0.57 μM (Hill coefficient n = 2) was obtained to the Hill equation using Grafit4 (Erithacus Software Ltd.). **(F)** mTrp peptide titration of TA-CaM_{1-80}. Conditions as in (E) except for 1 mM Ca^{2+} in the solution from the start. Upon mTrp additions of up to 600 nM to 30 nM TA-CaM_{1-80} there was a 2.8-fold fluorescence increase. Best fit K_d value of 360 ± 174 nM was obtained to the equation for the analysis of the binding curve representing bound versus total ligand concentrations using Grafit4 (Erithacus Software Ltd.) (excitation = 365 nm; emission = 420 nm).

Figure 9: 6ROX-CaM_{76-148} and 6ROX-CaM_{1-80} distributions in the presence of FL-WGA blocked nuclei and in the presence of FL-WGA not inhibiting nuclear transport. (A) & **(B)** HeLa cells were electroporated with 6ROX-CaM_{76-148} (left-hand panels) and FL-WGA (right-hand panels) in 2 mM EGTA. **(A)** When FL-WGA was incorporated into the nuclear membrane, 6ROX-CaM_{76-148} was found to be concentrated in the nucleus but none was present in the cytoplasm. Note the typical binding of 6ROX-

CaM_{76-148} to nucleoli and chromatin in low Ca^{2+} conditions. **(B)** When FL-WGA was not incorporated into the nuclear membrane, the 6ROX-CaM_{76-148} was 1.9-fold higher in the nucleus than in the cytoplasm as described above. **(C)** & **(D)** HeLa cells were electroporated with 6ROX-CaM_{1-80} (left-hand panels) and FL-WGA (right-hand panels) in 2 mM EGTA. **(C)** When FL-WGA was incorporated into the nuclear membrane, 6ROX-CaM_{1-80} was found to be concentrated in the nucleus but none was present in the cytoplasm. (D) When FL-WGA was not incorporated into the nuclear membrane, 6ROX-CaM_{1-80} was 1.4-fold higher in the nucleus than in the cytoplasm as described above.

Biochemical Journal Immediate Publication. Published on 16 Oct 2006 as manuscript BJ20061111

Figure 1

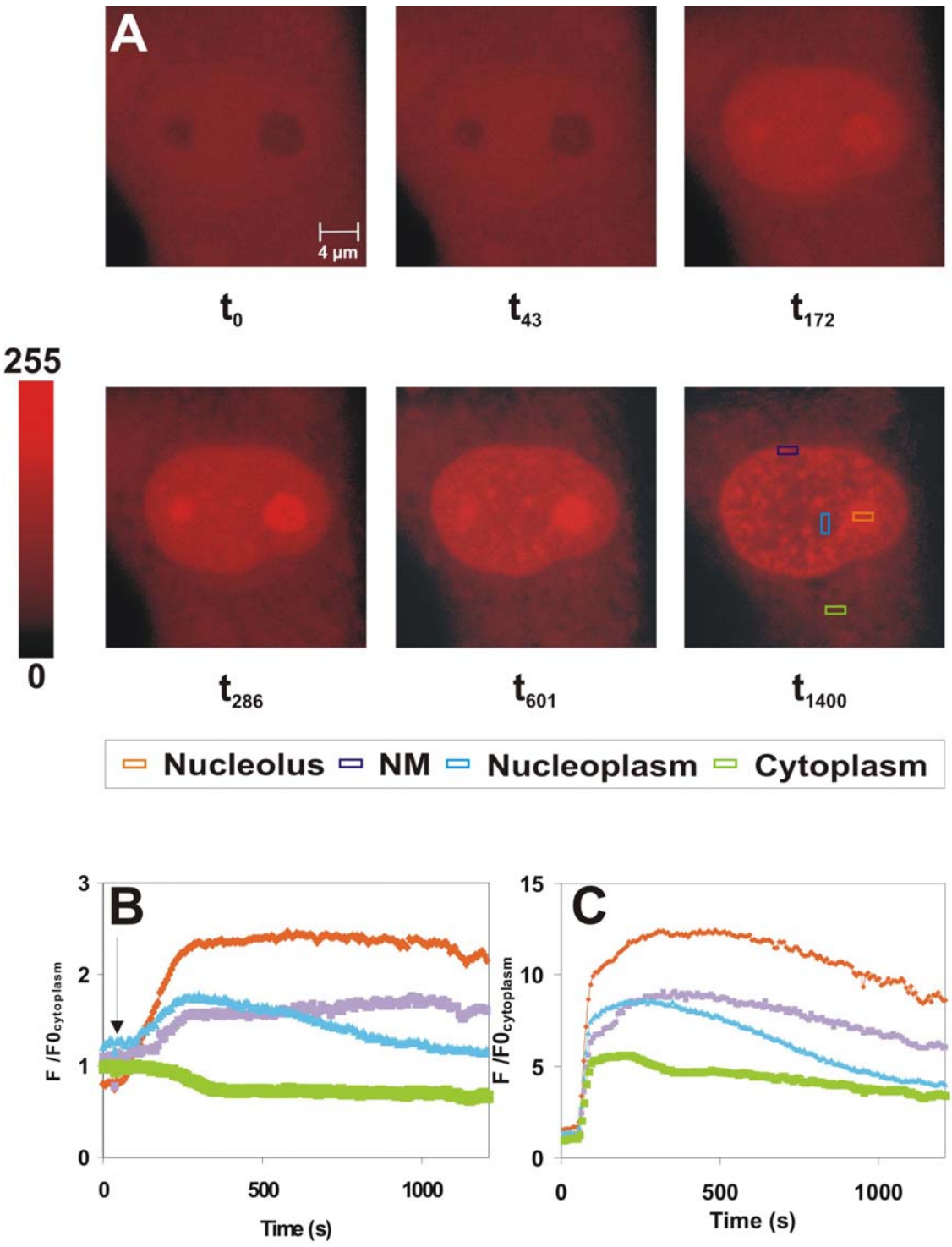

Biochemical Journal Immediate Publication. Published on 16 Oct 2006 as manuscript BJ20061111

Figure 2

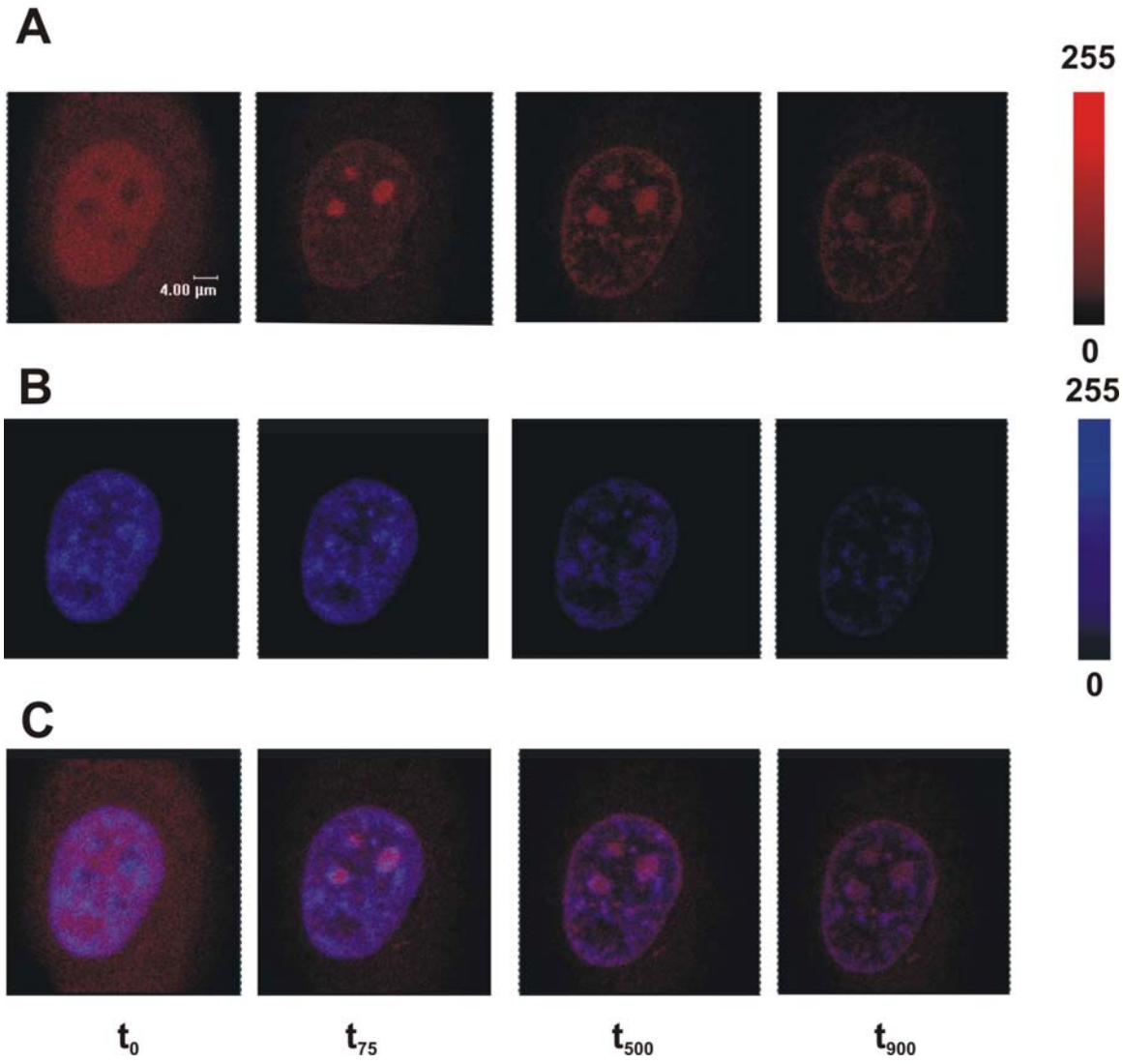

Biochemical Journal Immediate Publication. Published on 16 Oct 2006 as manuscript BJ20061111

Figure 3

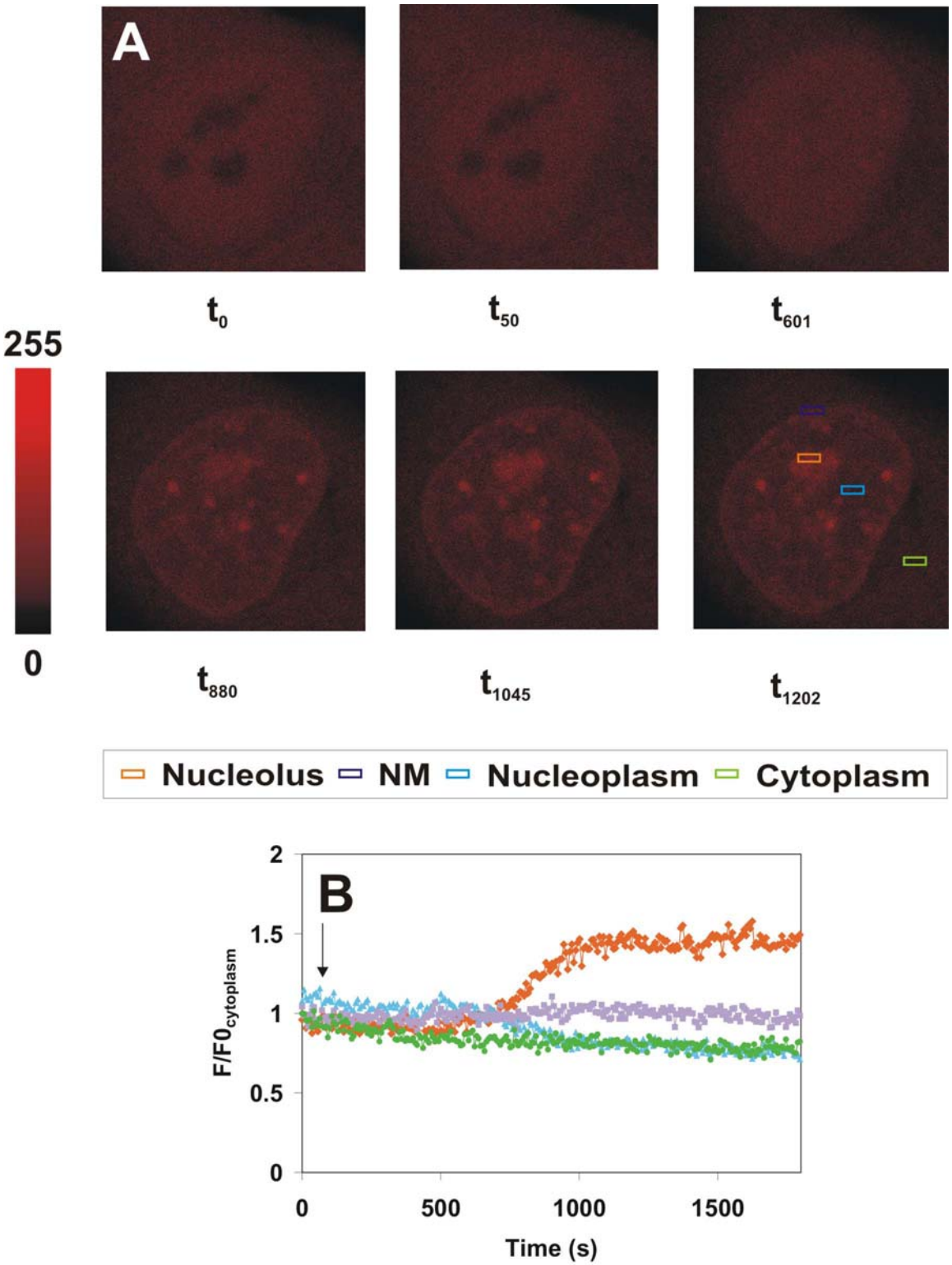

Biochemical Journal Immediate Publication. Published on 16 Oct 2006 as manuscript BJ20061111

Figure 4

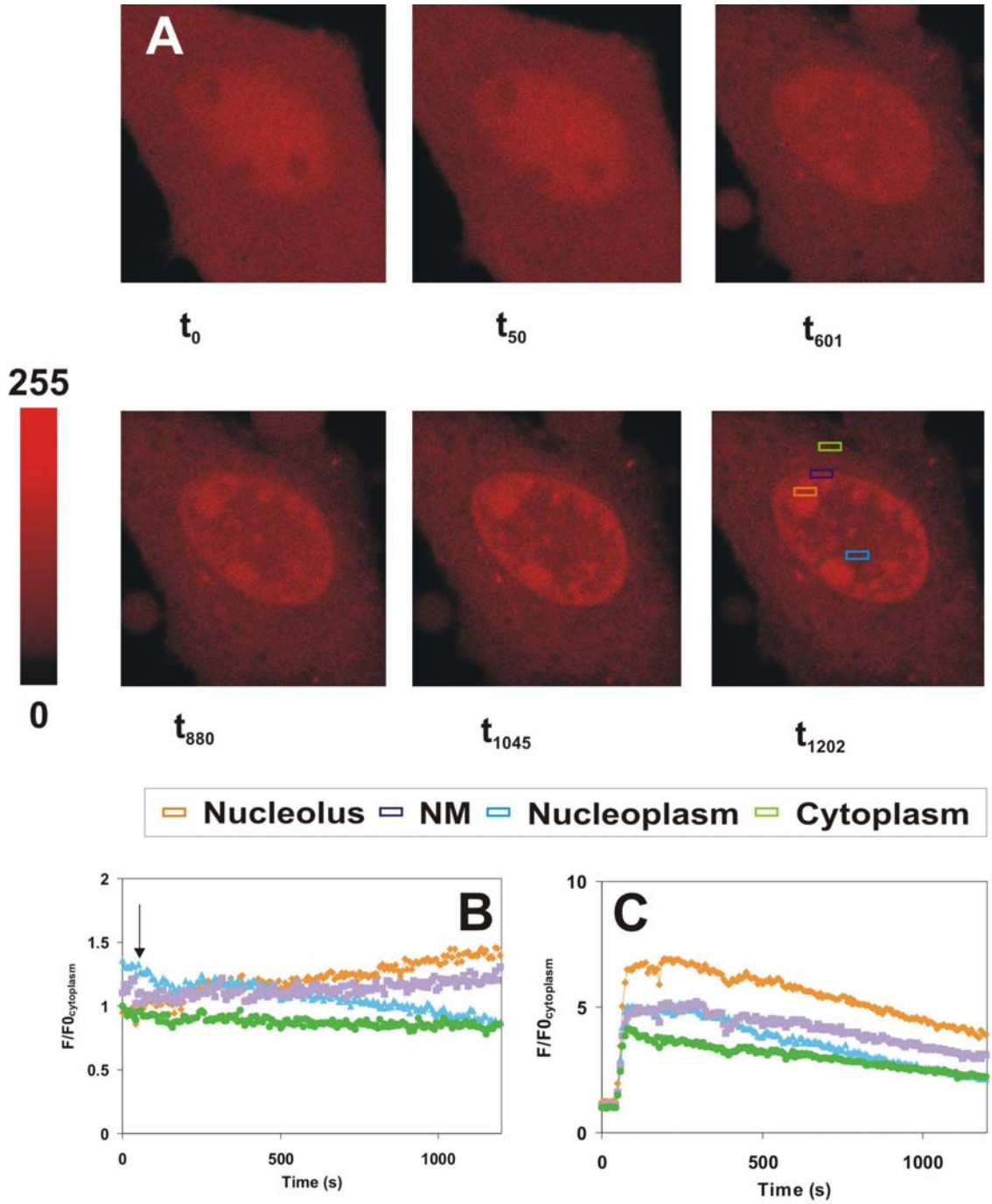

Biochemical Journal Immediate Publication. Published on 16 Oct 2006 as manuscript BJ20061111

Figure 5

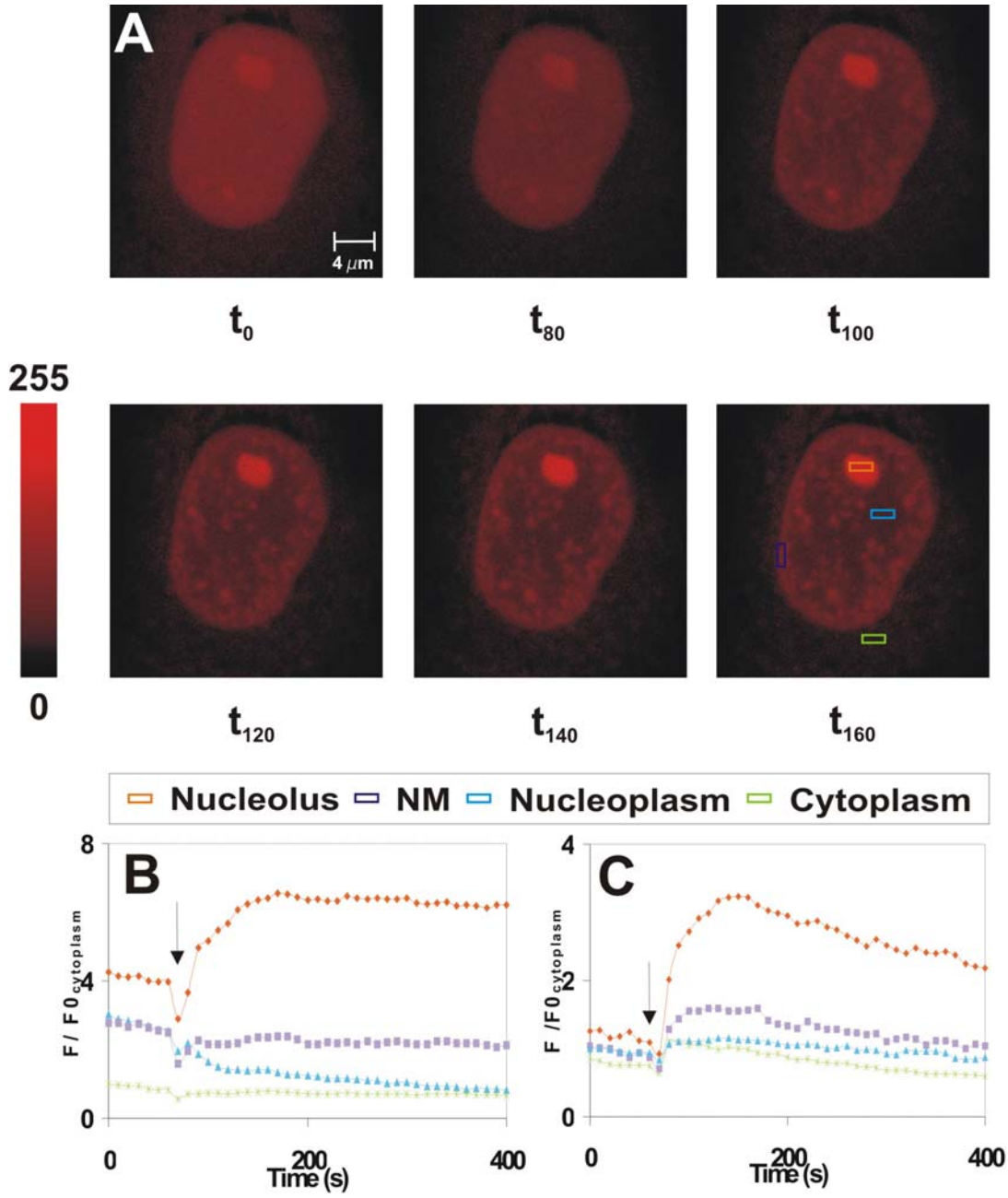

Biochemical Journal Immediate Publication. Published on 16 Oct 2006 as manuscript BJ20061111

Figure 6

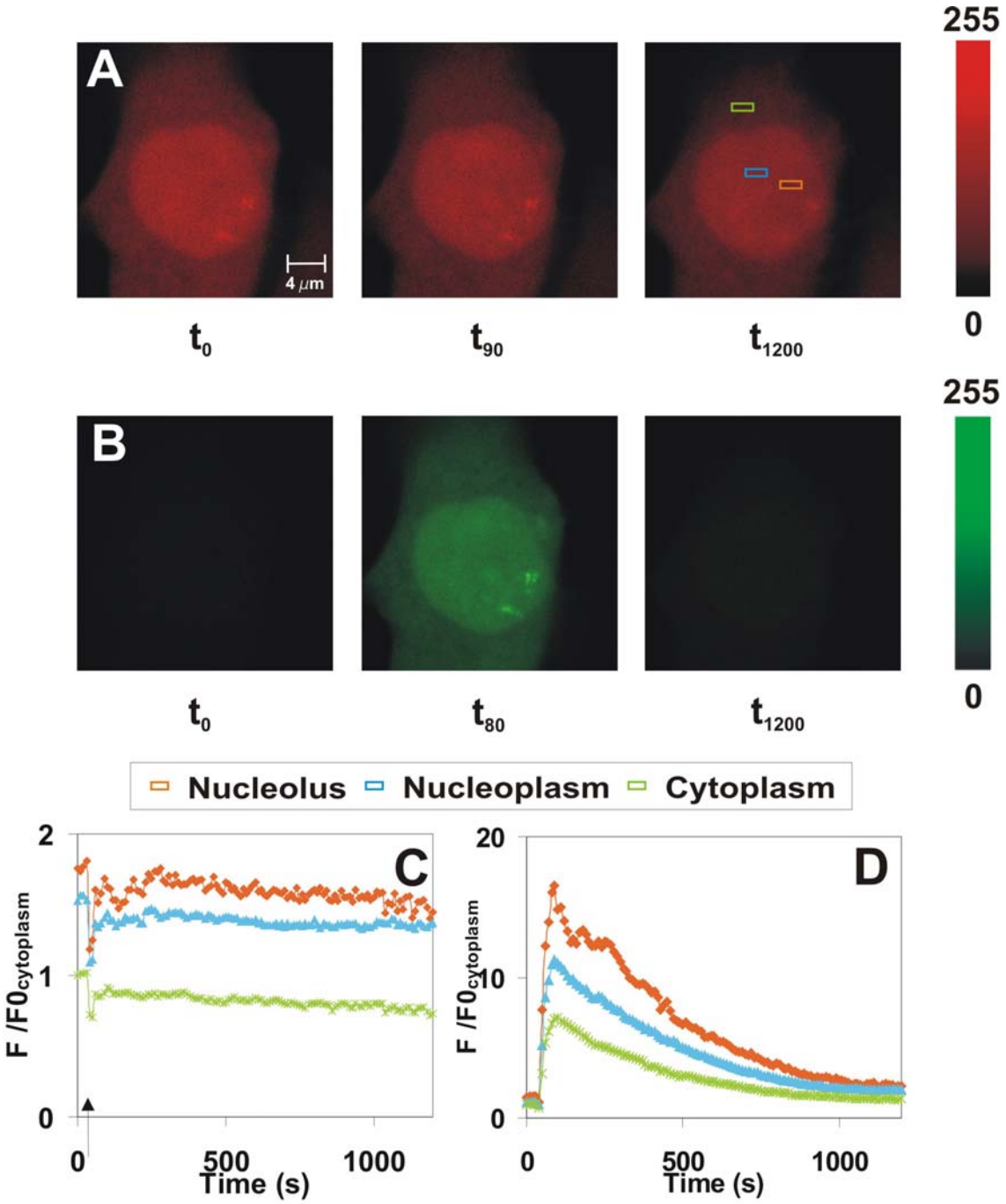

Biochemical Journal Immediate Publication. Published on 16 Oct 2006 as manuscript BJ20061111

Figure 7

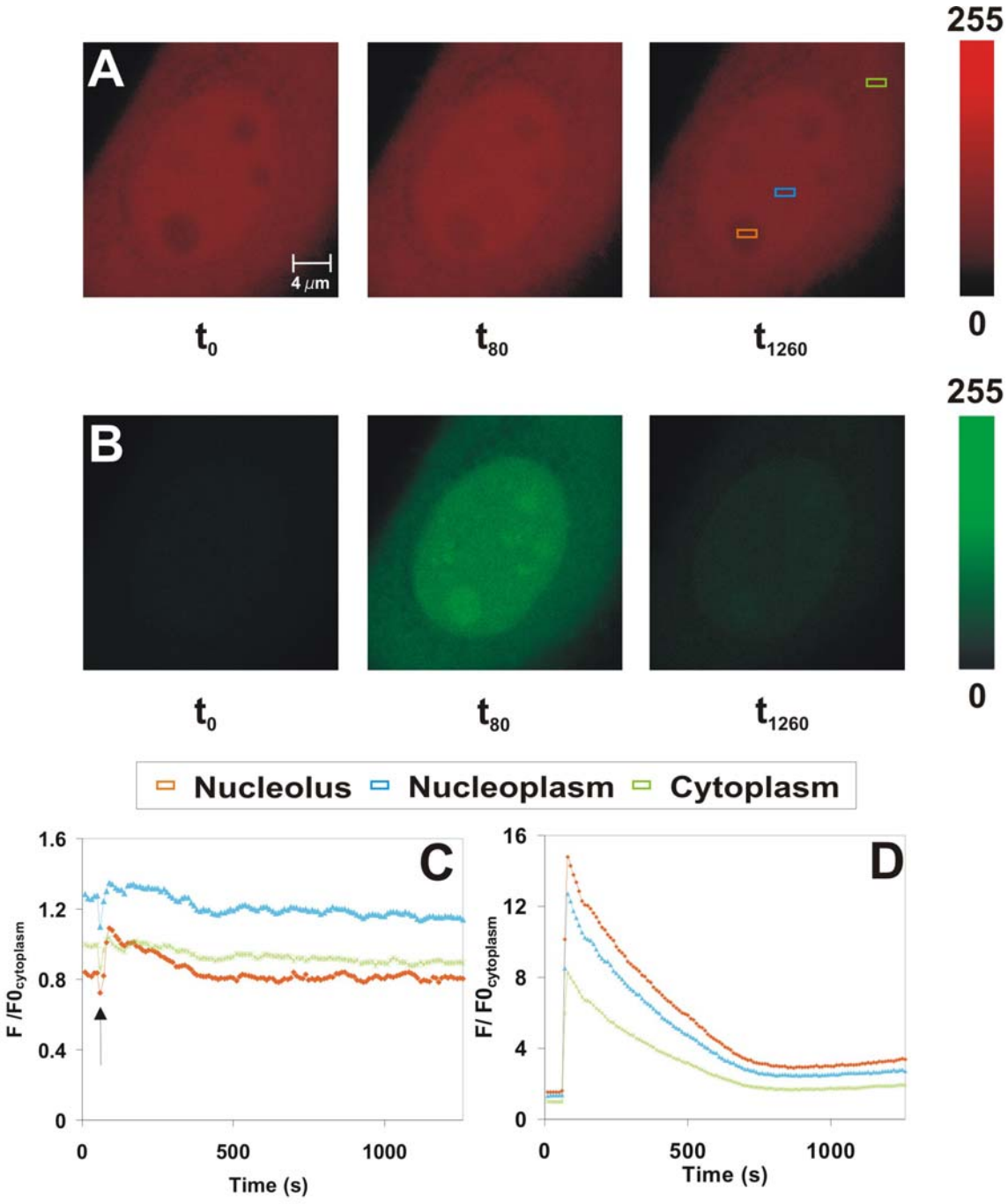

Biochemical Journal Immediate Publication. Published on 16 Oct 2006 as manuscript BJ20061111

Figure 8

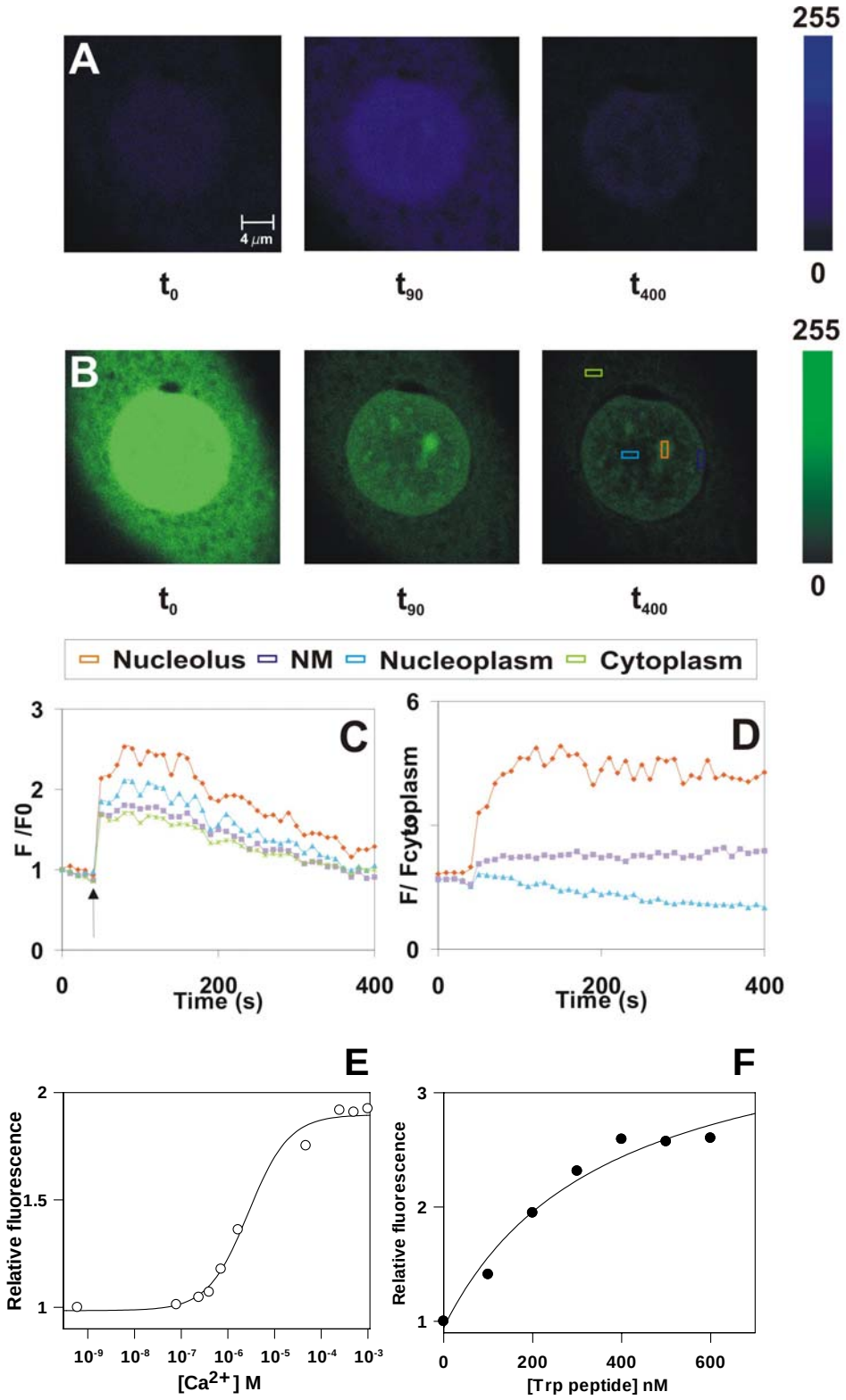

Figure 9